Supporting Information

Host-guest complexation in wide bandgap perovskite solar cells

Parnian Ferdowsi[1], Gianluca Bravetti[1–3], Moritz C. Schmidt[4], Efrain Ochoa-Martinez[1], Shanti Bijani[5], Aurora Rizzo[2], Silvia Calello[3], Ullrich Steiner[1], Bruno Ehrler[4], Dominik J. Kubicki[6], and Jovana V. Milić[1,*]*

[1]Adolphe Merkle Institute, University of Fribourg, 1700, Switzerland; [2]CNR NANOTEC – Istituto di Nanotecnologia, c/o Campus Ecotekne, Via Monteroni, 73100 Lecce, Italy; [3]CNR NANOTEC - c/o Dipartimento di Chimica, Università di Bari, Via Orabona 4, 70126 Bari, Italy; [4]Center for Nanophotonics, AMOLF, Science Park 104, 1098 XG Amsterdam, the Netherlands; [5]Unidad de Nanotecnología, Centro de Supercomputador y Bioinnovación SCBI, Universidad de Málaga, Calle Severo Ochoa 34, 29590 Campanillas (Málaga), Spain; Department of Physics, University of Warwick, Coventry, CV4 7AL, UK

Correspondence E-mail: parnian.ferdowsi@epfl.ch and jovana.milic@unifr.ch

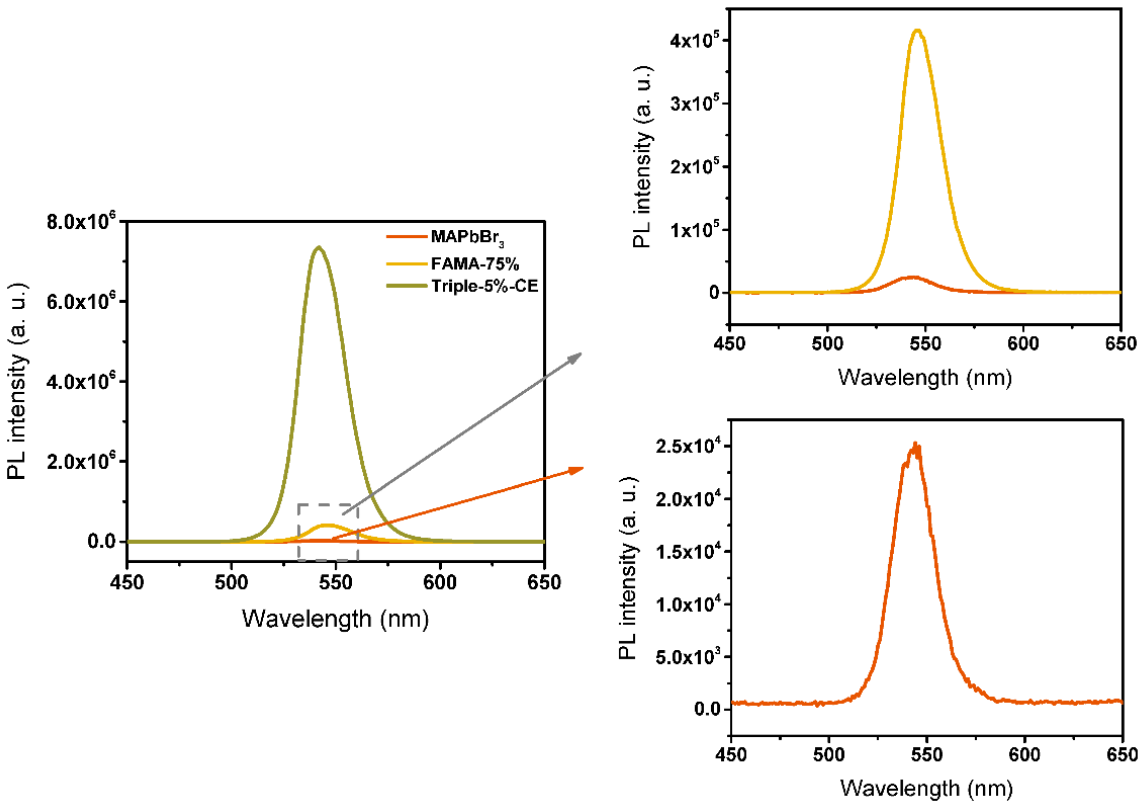

Figure S1. Photoluminescence spectra of single ($MAPbBr_3$), double ($FAMAPbBr_3$), and triple cation ($FAMACsPbBr_3$) perovskite films.

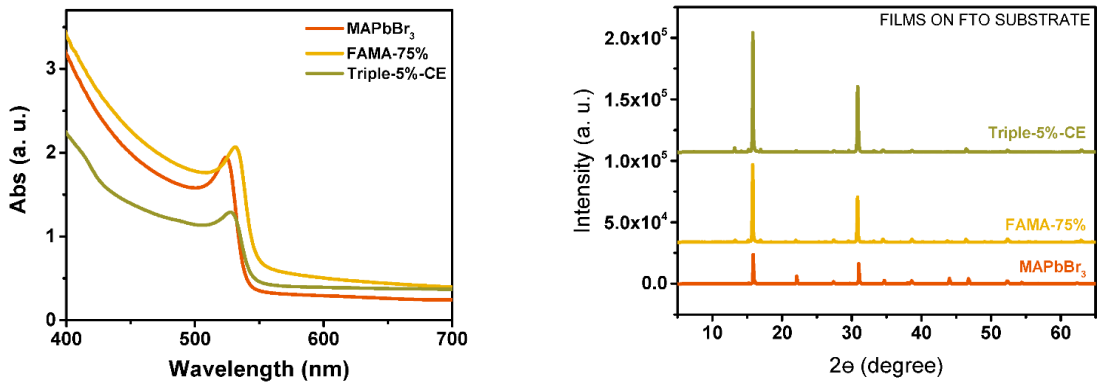

Figure S2. Absorption spectra (left) and XRD patterns (right) of single (MAPbBr3), double ($FAMAPbBr_3$), and triple cation ($FAMACsPbBr_3$) perovskite films.

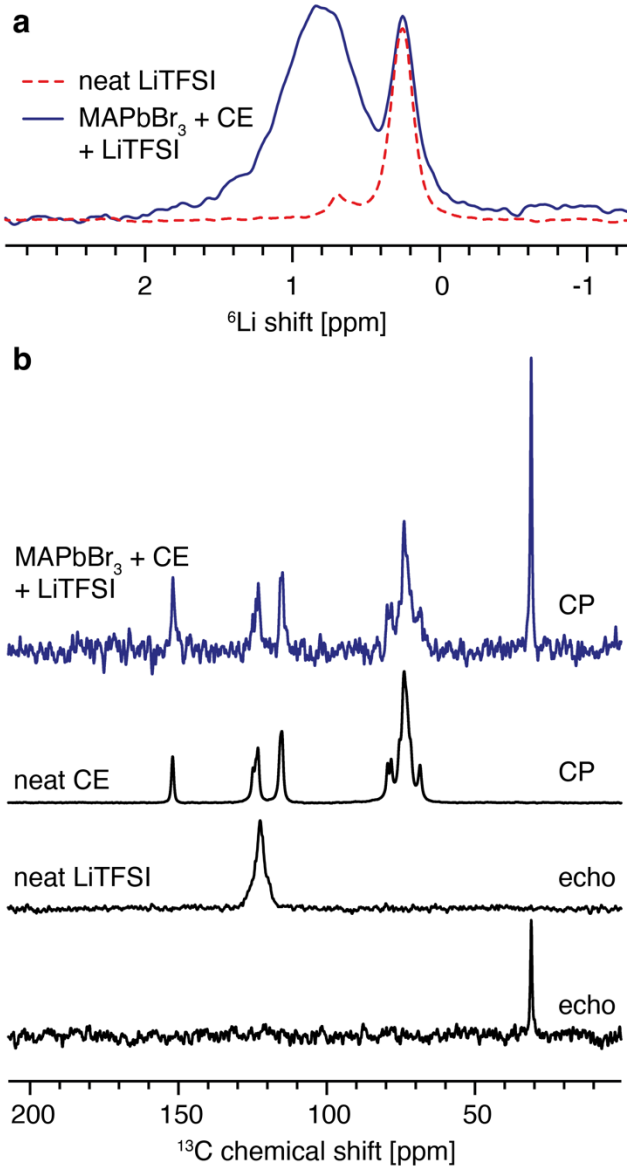

Figure S3. Solid-state MAS (a) ^{6}Li and (b) ^{13}C NMR spectra of $MAPbBr_3$ powders with and without LiTFSI compared with the neat samples of LiTFSI and CE.

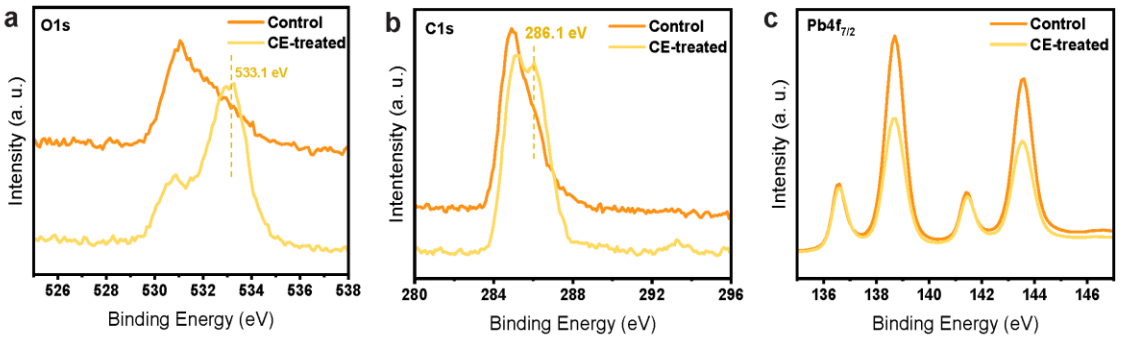

Figure S4. XPS spectra of control and CE-treated perovskite films in the range of (a) O 1s, (b) C 1s, and (c) Pb 4f core level peaks.

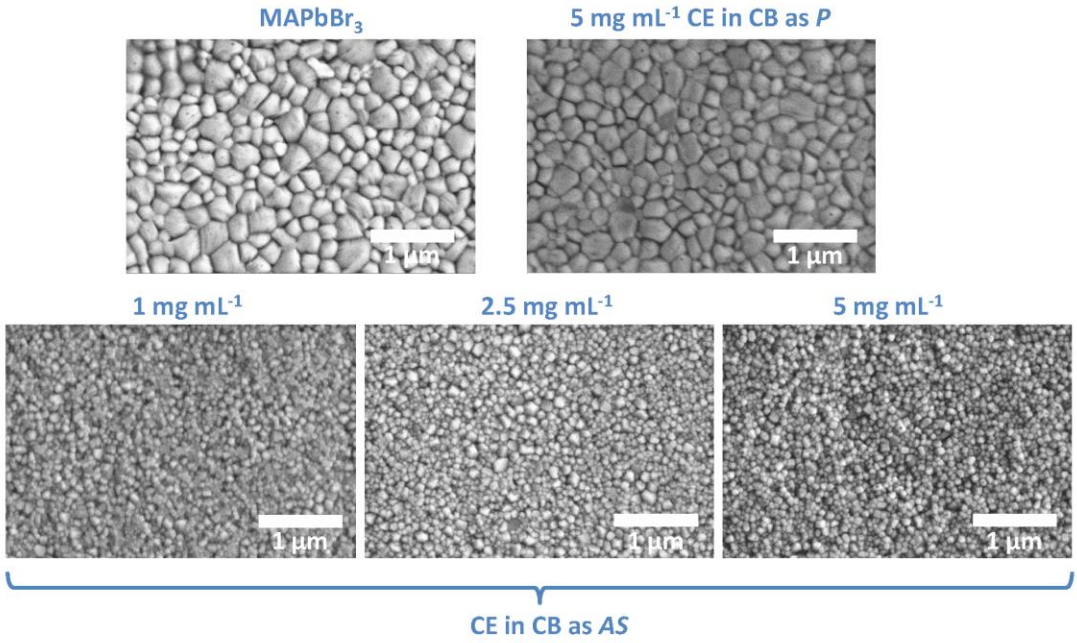

Figure S5. Top view SEM images of $MAPbBr_3$ prepared without/with CE treatment.

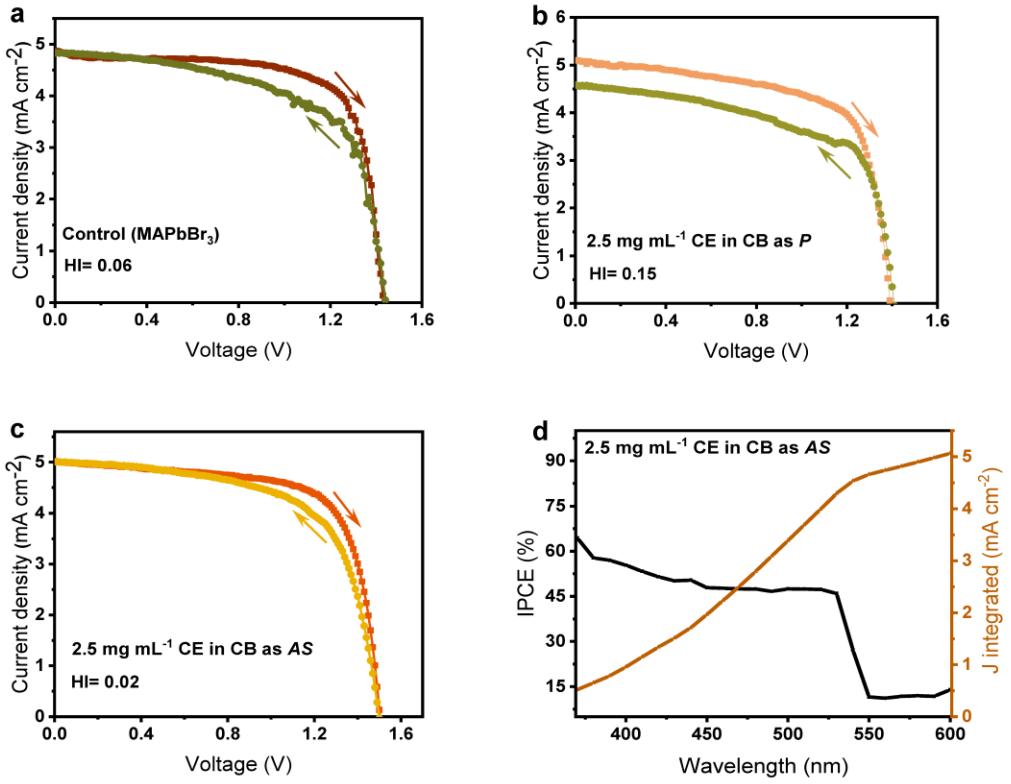

Figure S6. Current–voltage scans for the best-performing devices; (a) control, treated samples using CE prepared by (b) *P* and (c) *AS* method, (d) Incident photon-to-current efficiency (black, left ordinate) and photocurrent density (brown, right ordinate) calculated by integrating the IPCE with the AM1.5G solar spectrum. Hysteresis Index (HI) calculated using J_{RV} $(\frac{V_{OC}}{2})$-J_{FW} $(\frac{V_{OC}}{2})$ /J_{RV} $(\frac{V_{OC}}{2})$ equation.

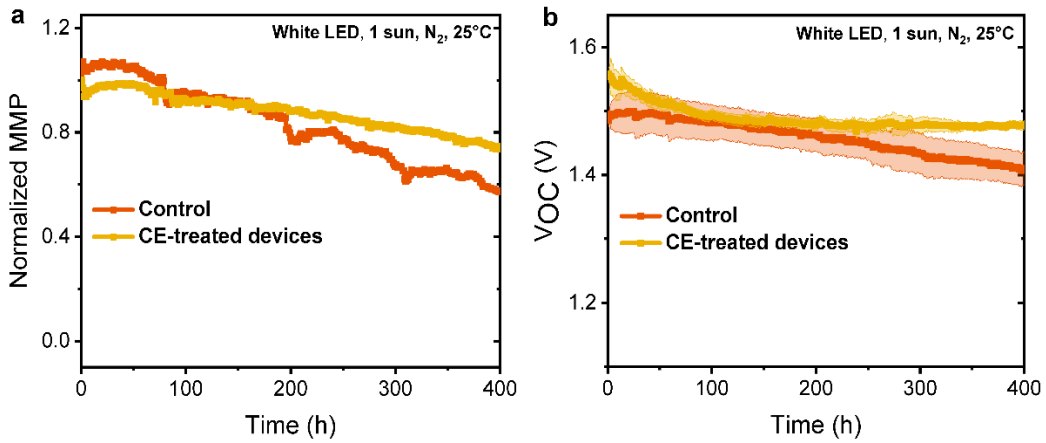

Figure S7. Ambient stability of PSCs with (yellow) and without (orange) CE treatment over 400 h at 25 °C in nitrogen flow, no encapsulation, no shadow mask, white LED without UV (1 sun) and no bias. The results are based on the evolution of the average PCE change.

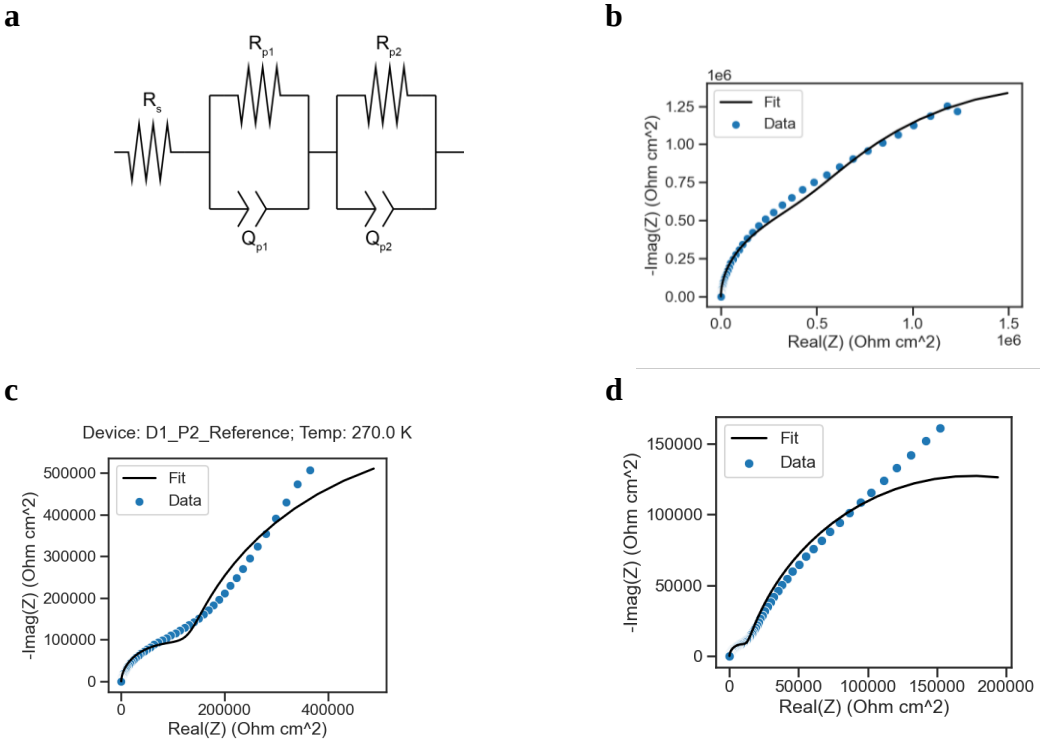

Figure S8. (a) Equivalent circuit to fit the impedance spectra. (b–c) Example fits of the impedance spectra of a reference device at (a) 216.0 K, (b) 270.0 K, and (c) 330.0 K.

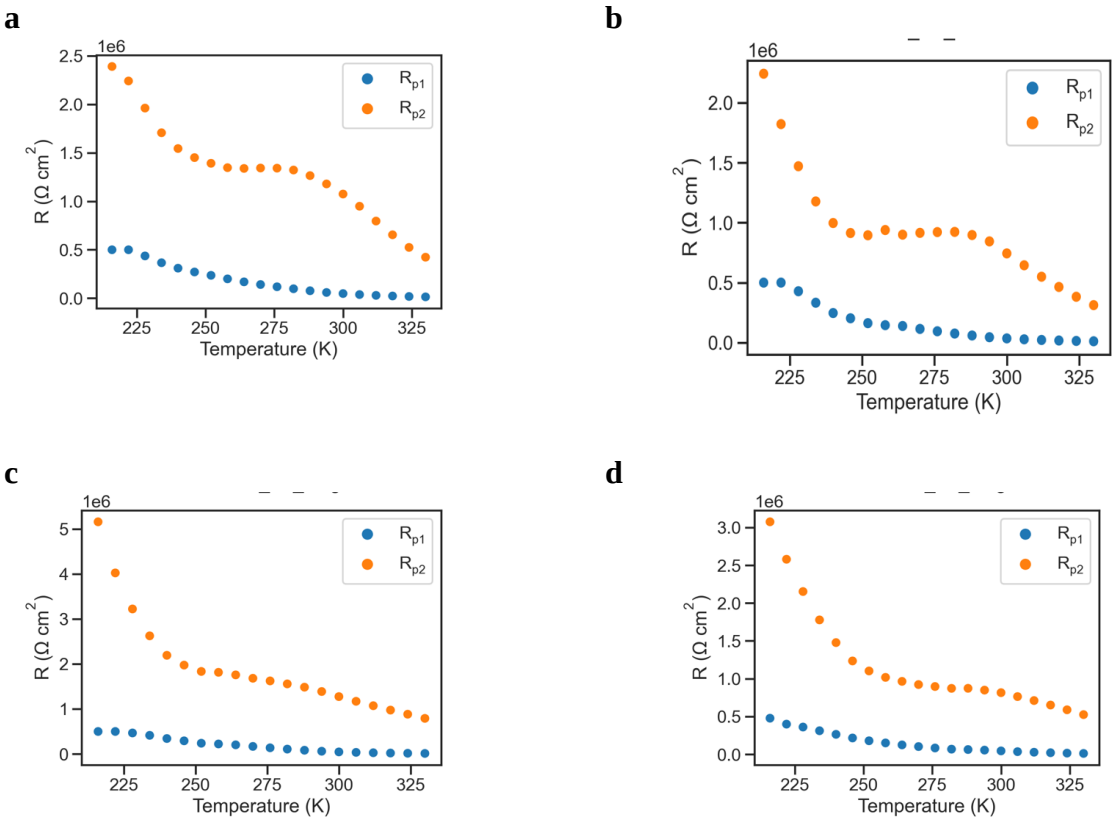

Figure S9. Extracted values for R_{p1} and R_{p2} at temperatures between 210.0 K and 330.0 K; (a) and (b) contain values of reference devices, while (c) and (d) contain values of treated devices.

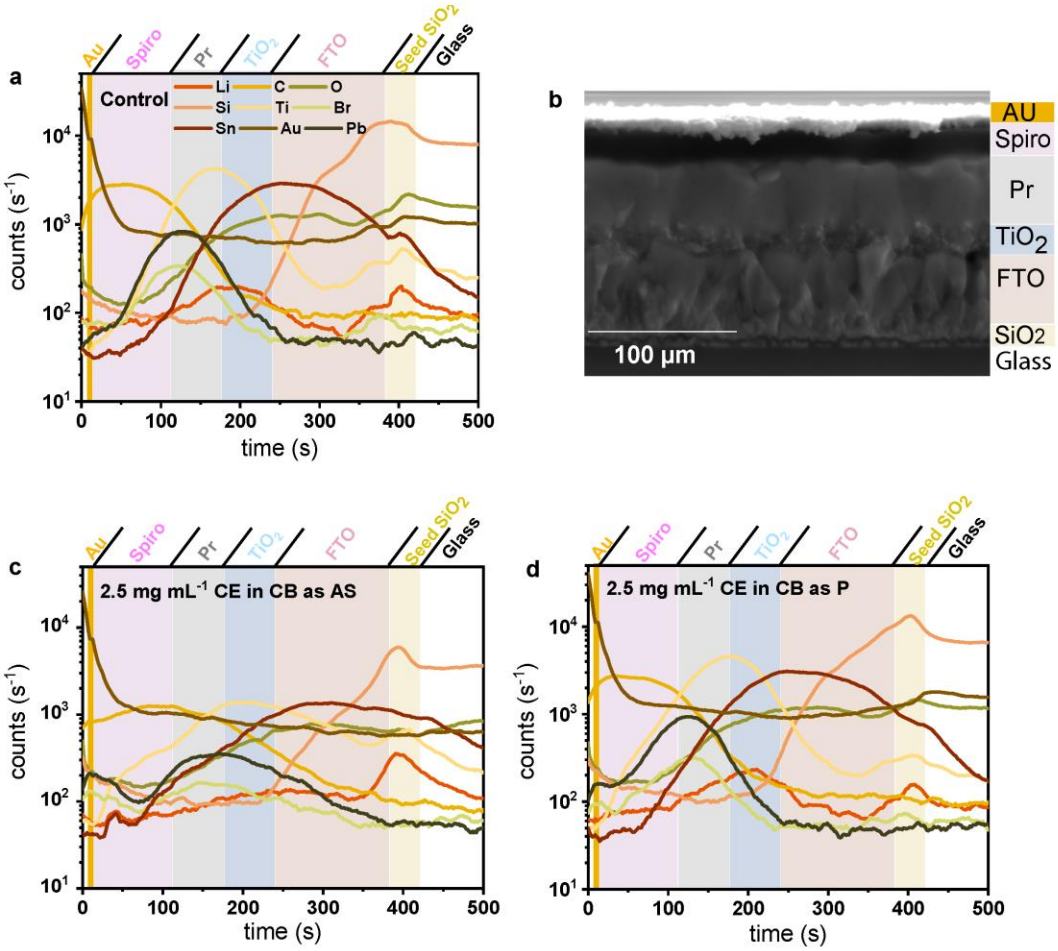

Figure S10. Depth profile analysis of $MAPbBr_3$ samples; (a) control, (b) cross-section SEM image of $MAPbBr_3$, treated samples using CE prepared by (c) *AS* and (d) *P* method.

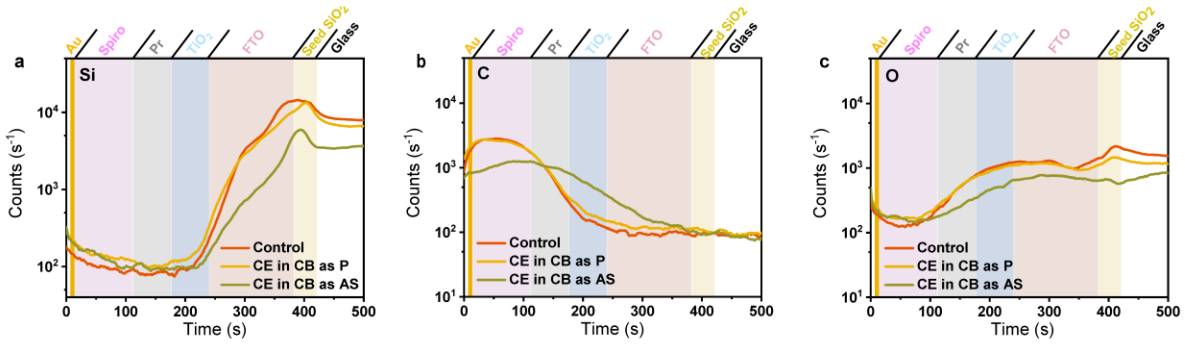

Figure S11. Light elements depth profiles obtained for the analysis of $MAPbBr_3$ samples by SNMS. Control and treated samples using CE prepared by *AS* and *P* method; (a) Si, (b) C, and (c) O.

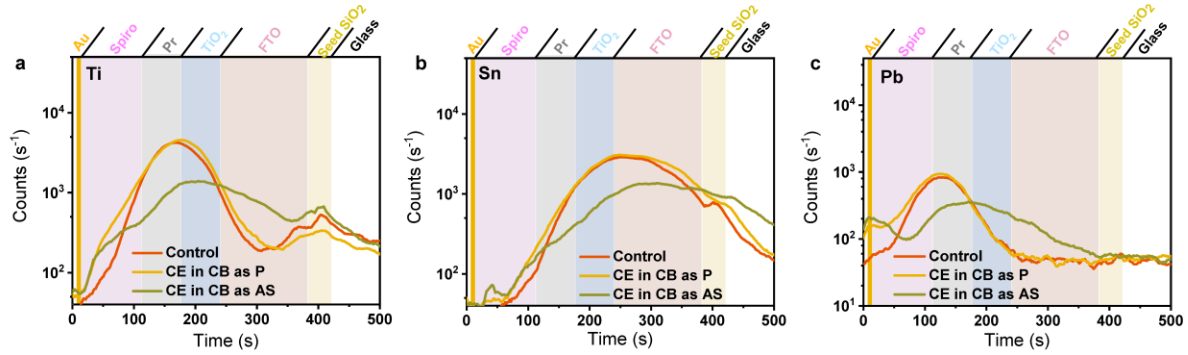

Figure S12. Heavy elements depth profiles obtained for the analysis of $MAPbBr_3$ samples by SNMS. Control and treated samples using CE prepared by *AS* and *P* method; (a) Ti, (b) Sn, and (c) Pb.

Table S3. Photovoltaic parameter data of treated devices (*AS*) in different concentrations.

Variables	V_{OC} (V)	J_{SC} (mA cm^{-2})	FF	PCE%

Table S1. Photovoltaic parameter data of representative devices based on different compositions.

Variables	V_{OC} (V)	J_{SC} (mA cm^{-2})	FF	PCE%
$MAPbBr_3$	1.40±0.01	5.54±0.18	71.63 ±4.5	5.47±0.33
$FA_{0.75}MA_{0.25}PbBr_3$	1.12±0.06	3.67±0.42	43.08±6.9	1.81±0.48
$Cs_{0.05}(FA_{0.75}MA_{0.25})_{0.95}PbBr_3$	1.06±0.03	1.88±0.23	37.35±8.4	0.77±0.24
Remeasurement five days after metal evaporation				
$MAPbBr_3$	1.46±0.02	5.58±0.24	67.47±4	5.49±0.27
$FA_{0.75}MA_{0.25}PbBr_3$	1.01±0.09	4.18±1.36	37.93±4.9	1.82±0.64
$Cs_{0.05}(FA_{0.75}MA_{0.25})_{0.95}PbBr_3$	0.96±0.02	0.73±0.1	34.2±0.87	0.25±0.05

Table S2. Variation of (100) and (200) peaks Full Width at Half Maximum (FWHM) and crystal size with CE treatment.

Variables	2θ	FWHM	Crystallite size from Scherrer equation (nm)
CE in CB as *AS*			
$MAPbBr_3$ + CE (1 mg mL^{-1})	15.85	0.21	38.40
	31.02	0.23	36.41
$MAPbBr_3$ + CE (2.5 mg mL^{-1})	15.82	0.10	79.12
	30.99	0.15	55.78
$MAPbBr_3$ + CE (5 mg mL^{-1})	15.84	0.09	87.08
	31.01	0.14	60.54
CE in CB as *P*			
$MAPbBr_3$ + CE (1 mg mL^{-1})	15.92	0.09	85.95
	31.10	0.14	58.13
$MAPbBr_3$ + CE (2.5 mg mL^{-1})	15.93	0.09	85.15
	31.11	0.14	57.11
$MAPbBr_3$ + CE (5 mg mL^{-1})	15.94	0.12	68.88
	31.09	0.13	65.77
$MAPbBr_3$	1.41±0.01	4.68±0.47	69.01 ±11.77	4.51±0.72
$MAPbBr_3$ + CE (1 mg mL^{-1})/*AS*	1.47±0.21	5.24±0.22	61.72±4.92	4.76±0.50
$MAPbBr_3$ + CE (2.5 mg mL^{-1})/*AS*	1.48±0.18	5.18±0.12	63.77±4.42	4.89±0.36
$MAPbBr_3$ + CE (5 mg mL^{-1})/*AS*	1.42±0.20	4.26±0.40	51.67±4.26	3.11±0.28

Reference

1. M. H. Futscher, J. M. Lee, L. McGovern, L. A. Muscarella, T. Wang, M. I. Haider, A. Fakharuddin, L. Schmidt-Mende, B. Ehrler, *Mater. Horiz.* **2019**, *6*, 1497. Quantification of Ion Migration in $CH_3NH_3PbI_3$ Perovskite Solar Cells by Transient Capacitance Measurements.

2. M. V. Pelarda, B. C. Hames., I. G-Benito, O. Almora, A. M-Ontoria, R. S. Sánchez, G. G-Belmonte, N. Martín, I. M-Sero, *J. Phys. Chem. Lett*. **2016**, *7*, 22, 4622. Analysis of the Hysteresis Behavior of Perovskite Solar Cells with Interfacial Fullerene Self-Assembled Monolayers.